Available online at www.sciencedirect.com
ScienceDirect
European Journal of Operational Research 182 (2007) 640–662
EUROPEAN JOURNAL OF OPERATIONAL RESEARCH
www.elsevier.com/locate/ejor

Discrete Optimization

Microscopic modeling and control logic for incident-responsive automatic vehicle movements in single-automated-lane highway systems

Jiuh-Biing Sheu *

Institute of Traffic and Transportation, National Chiao Tung University, 4F, 114 Chung Hsiao W. Rd., Sec. 1, Taipei, Taiwan 10012, ROC

Received 8 April 2005; accepted 22 August 2006
Available online 29 November 2006

Abstract

Automatic response to lane-blocking incidents is a critical issue in the field of automated highway systems (AHS). Accordingly, this paper presents a microscopic vehicular control methodology for automatic-control (AC) vehicular movements in response to lane-blocking incidents in the AHS environment. The embedded traffic control logic is based on the basic safety requirements for automatic-control lane traffic maneuvers responding to lane-blocking incidents in the single-automated-lane AHS environment. Accordingly, respective automated vehicular control models are proposed to deal with AC vehicles moving in three corresponding sequential phases, i.e., (1) AC platoon approaching the incident site from the blocked lane, (2) mandatory lane changing and mixed car following in the adjacent lane, and (3) AC platoon reforming downstream from the incident site in the blocked automated lane. Using a microscopic simulation model which embeds these proposed models, preliminary tests are conducted to investigate the relative performance of the proposed method in various traffic flow and control scenarios. The resulting numerical results, including simplified sensitivity analyses, indicate that the proposed microscopic traffic control logic permits regulating automatic-control vehicular movements in response to the effects of lane-blocking incidents on traffic flows either in control-free lanes or in the automatic-control lanes. Implications of the results and some findings are discussed for further research.

Keywords: Traffic; Microscopic modeling; Automatic-control vehicles; Incident-responsive

1. Introduction

Prompt response to lane-blocking incidents is a critical issue in the development of advanced automated highway systems (AHS) although all the limited existing AHS technologies are on trial. In this paper, a lane-blocking incident in AHS refers to any lane blockage in either the automated-control lanes or the

* Tel.: +886 2 2349 4963; fax: +886 2 2349 4953.
E-mail address: jbsheu@mail.nctu.edu.tw

0377-2217/$ - see front matter
doi:10.1016/j.ejor.2006.08.053

adjacent control-free lanes on AHS freeways. Such a lane-blocking incident may be caused by any unusual event, e.g., malfunction of automatic control systems in automated vehicles, or abnormal traffic conflicts resulting from the traffic flows in adjacent lanes in either the single-automated-lane or multi-automated-lane AHS environment. The significance of this issue can be perceived from three aspects. First, the phenomena of incident-induced lane traffic maneuvers, including mandatory lane changing and queue overflowing, actually remain ambiguous in numerous related study fields, e.g., traffic theory, incident management, and traffic control. Other relevant discussions can be readily found in our previous literature (Sheu et al., 2001; Sheu and Ritchie, 2001b; Sheu, 2002, 2003a,b). Second, the traffic maneuvers of automatic-control (AC) vehicles are different from those of AC-free vehicles, which rely primarily on human factors. Consequently, the effects of incidents on the mixed traffic flows are more complex than those on the existing fully AC-free traffic flows, given the exclusive AHS lanes existing in the normal freeway systems. Thirdly, the variety of incident characteristics (e.g., incident duration and location) coupled with incident impacts (e.g., delays and queue lengths) in both the temporal domain and the spatial domain have led to the invalidation of the existing traffic control and management strategies, which may further contribute to the uncertainty surrounding the system performance of AHS. One might argue that the aforementioned reasoning may not hold in the case of fully AC traffic flows where each vehicle is supposed to be ideally controlled. Nevertheless, the incident-responsive strategies remain unknown in the above ideal scenario.

Although recent years have seen growing advances in investigating AHS traffic flow problems and the corresponding control logic rules, investigation of the corresponding AHS lane traffic maneuvers and respective control logic to address the issues of AHS under anomalous operational conditions appear to warrant more research effort. Some typical examples are illustrated below for further discussion.

The control system architecture and corresponding functionality of intelligent vehicle/highway systems were amplified in Varaiya (1993), which provides an elaborate overview of AHS. According to the description in Broucke and Varaiya (1996), vehicles in the AHS environment might be under automatic control in terms of the corresponding traffic maneuvers, e.g., the vehicular headways in a given platoon, the spacing between two sequential platoons, platoon-based speeds, and the route from entry into the highway to exit. All the aforementioned traffic attributes should be determined automatically by specific control logic, e.g., optimal control. Given the fully automatic control condition, Hall and Lotspeich (1996) proposed a linear programming model to deal with the lane traffic assignment problem on an automated highway with the goal of maximizing the total throughput. However, the assumptions in terms of vehicular lane changing and corresponding formulas coupled with lane-changing coefficients may not hold true in lane-blocking incident cases. Similar problems are also found in Li and Wang (2002), which investigated a simplified automated lane-changing control model based on the concept of fairly distributing lane densities. Although the problems of bottlenecking at ramps of an AHS freeway have been investigated by some researchers (Ran et al., 1996; Zhang, 1996), their solution strategies appear to be inapplicable for mainline lane-blocking incident cases; and furthermore, the characterization of AHS traffic flows at bottlenecks remained vague in the literature. Efforts of other researchers devoted to controlling AHS platoons against longitudinal and lateral collisions via novel control technologies, e.g., fuzzy logic control and hierarchical hybrid control, can also be found in the literature (Godbole, 1994; Hessburg, 1994; Seto and Inoue, 1999). Nevertheless, the applicability of these methods in incident scenarios still remains problematic. In addition, several specific simulators which embed AHS traffic flow models were proposed to analyze the traffic dynamics of AHS in various traffic scenarios (Eskafi et al., 1995; Haddon, 1997; Gollu and Varaiya, 1998). However, there are limited numerical results to verify the validity of these resulting AHS traffic simulation models under lane-blocking incident conditions.

In addition, the resulting AHS emergency management maneuvers and related simulation experimental design have also raised increasing research interests (Ioannou, 1998; Lygeros et al., 2000; Yi et al., 2001; Toy et al., 2002). For instance, considering the issues of safety and human factors existing in the scenario of automated vehicle movements mixed with manually-driven vehicles, scenario design and evaluation via simulation were conducted in Ioannou (1998), which concludes that several safety concerns may still remain in the interaction of fully automated vehicles with manually-driven ones due to unpredictable maneuvers of drivers of those manual vehicles. Extended from the control hierarchy of Varaiya (1993), a fault tolerant control framework, which includes several control layers, is proposed in Lygeros et al. (2000) to deal with the operations of AHS under diverse faulty conditions, e.g., vehicular malfunction, infrastructure failure, and

driver-vehicle interaction failure. Yi et al. (2001) further integrated the functions of fault diagnostics and fault management to enhance the performance of AHS in longitudinal control. Aiming at Given two or more AHS lanes without the interruption of manually-driven vehicles, specific AHS traffic control laws coupled with three emergency vehicle maneuvers were proposed in Toy et al. (2002) to quickly respond to the faulty conditions of AHS. Using both the SmartAHS microscopic and SmartCap meso-scopic traffic simulators, their numerical results indicated that through elaborate degraded mode control logic together with emergency vehicle transit maneuvers, the AHS may recover efficiently from faults.

Due to the significance of the aforementioned faulty AHS issues, and the necessity of more research effort to explore the potential effects and solutions, we propose a microscopic traffic model together with AC vehicular control logic rules to investigate the potential AHS lane traffic maneuvers to automatically respond to the condition of lane-blocking incidents on single automated-lane freeways. Considering the complexity and diversity of the aforementioned problems in different operational scenarios, the present study scope may aim merely at the cases of lane-blocking incidents on single-automated-lane highways. Given that a lane-blocking incident on the single-automated-lane of a multi-lane freeway is identified, the intra-lane and inter-lane AC vehicular maneuvers automatically responding to the given lane-blocking incident are formulated with respective microscopic traffic models, and followed by the development of specific control logic rules embedded in the proposed algorithm. The corresponding procedures of methodology development are detailed below.

2. System specification

The proposed microscopic incident-induced AC traffic model involves two major components: (1) intra-lane traffic behavior modeling, and (2) inter-lane traffic behavior modeling. Herein, the former aims to characterize the potential AC platoon-decomposition maneuvers when a given AC platoon is approaching a given incident site; the latter is proposed to deal with lane-changing maneuvers of decomposed AC vehicles both upstream and downstream from the incident site for the re-composition of an AC platoon.

To characterize the aforementioned incident-induced intra-lane and inter-lane AC traffic maneuvers, the concept of an incident-impacted zone, referring to the area within which any given AC platoon is influenced by the given incident, is introduced. Correspondingly, under the proposed control logic, any given AC platoon within the incident-impacted zone is forced to follow the aforementioned two types of AC lane traffic maneuvers in order to pass smoothly by the incident site. Given a specific incident-impacted zone, as illustrated in Fig. 1, let us consider three potential scenarios, including (1) platoon-approaching, (2) lane-changing, and (3) platoon-reforming, which mimic the aforementioned lane traffic maneuvers potentially conducted by a given AC platoon in the incident-impacted zone. In the first scenario, the approaching AC platoon may adjust its approaching speed in response to the potential incident impact ahead; and meanwhile start out to decompose itself into disaggregated AC vehicles. In the second scenario, these disaggregated AC vehicles may trigger the automated lane-changing mechanism to pass by the incident site via the adjacent lane, given that the traffic flow condition in the adjacent lane is allowed. Otherwise, these decomposed AC vehicles should stand by in the blocked automated lane upstream from the incident site until the lane-changing maneuver is permitted. Once the AC vehicles pass by the incident site, they may execute the lane-changing maneuver back from the adjacent lane to the automated-control lane in the third scenario, and then reform a new platoon to continue their routing on the automated lane of the freeway. All the aforementioned traffic maneuvers are supposed to be completed within the given incident-impacted zone. Note that those AC platoons outside the incident-impacted zone are free from the specific incident-responsive control, and thus can follow any published AHS control logic to continue their routing operations.

In addition, two basic assumptions are postulated to facilitate model formulation. They are summarized as follows.

(1) All the AC vehicles are equipped with advanced communication/detection technology, e.g., in-vehicle computers and sensors, to have access to the instantaneous states of all the surrounding vehicular movements including the manually-driven vehicles in the adjacent lane and incident characteristics.

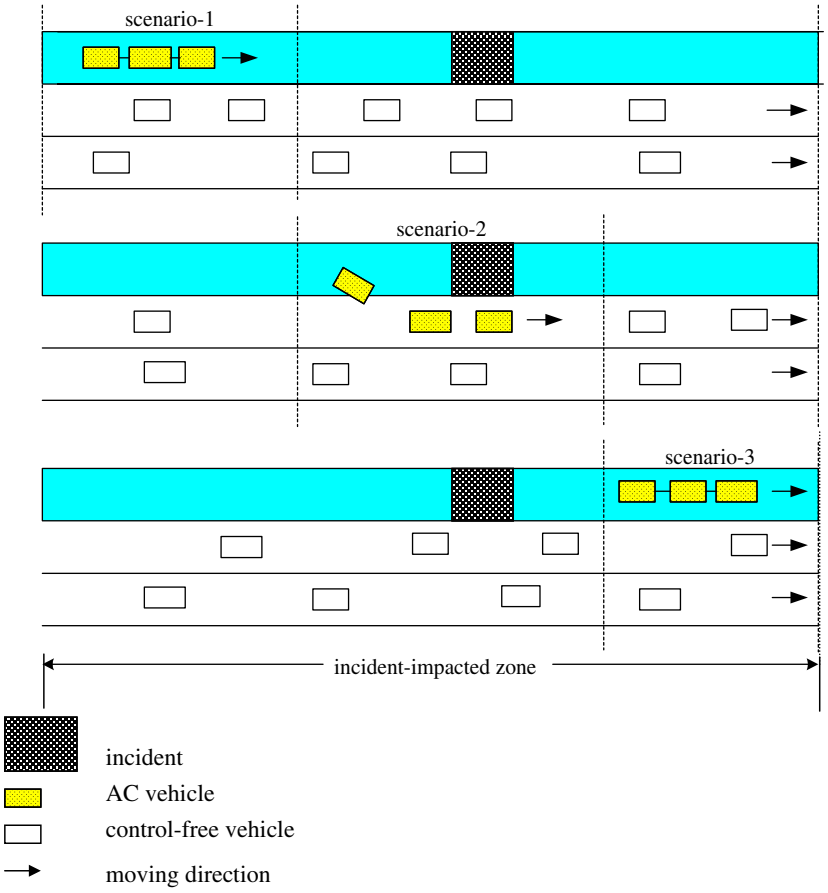

Fig. 1. Illustration of an incident-impacted zone.

(2) Each AC vehicle is assumed to follow the resulting computational commands instantaneously. The details of formulating the incident-induced lane traffic maneuvers, together with the corresponding control logic in the aforementioned three sequential scenarios, are presented in the following sections.
(3) All the auxiliary infrastructure including roadside/on-road devices is assumed to be ideally installed to assist the fulfillment of the proposed incident-responsive AC platoon maneuvers.

3. Platoon-approaching maneuvers

To control the intra-lane AC platoon maneuvers approaching the incident site, three types of dynamic zones are specified to determine the maneuvers of (1) platoon decomposing, (2) incident-induced AC car following, and (3) mandatory braking, respectively. The aforementioned three types of dynamic zones are bounded by three spatial thresholds: X_{d}^{σ}, X_{f}^{σ} and X_{b}^{σ}, referring to three critical longitudinal distances upstream from the incident site used to regulate the maneuvers of a given target AC platoon σ in terms of (1) platoon decomposing (coded d for short), (2) car following (coded f for short), and (3) mandatory braking (coded b for short), respectively. These thresholds are dynamically determined each time when any given AC platoon approaching to the incident site is observed. Fig. 2 illustrates these time-varying boundaries together with the corresponding AC traffic maneuvers, and the derivations associated with X_{d}^{σ}, X_{f}^{σ} and X_{b}^{σ} are described below.

X_{b}^{σ} is derived primarily on the consideration of the minimum spatial requirement that permits all the AC vehicles decomposed from the targeted platoon σ to stop safely in front of the incident site, given that

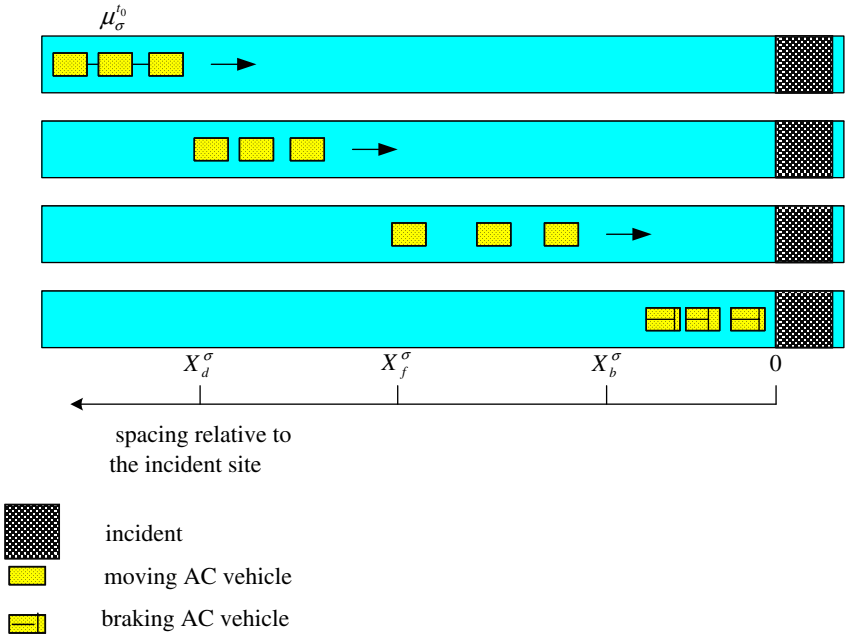

Fig. 2. Dynamic spatial thresholds for approaching AC platoon maneuvers.

vehicular lane-changing maneuvers are not allowed in the previous car-following scenario. In addition, the potential accumulated queue length formed by the remaining vehicles of the front AC platoon should also be taken into account. Here let us consider "$n_\sigma^{t_b}$" units of approaching AC vehicles of the targeted platoon σ, which are supposed to enter into the mandatory-braking area with the approaching speed $\mu_\sigma^{t_b}$ at time t_b, given that there are instantaneous "$n_{\sigma-1}^{t_b}$" units of AC vehicles of the front platoon (coded with $\sigma - 1$) queuing ahead of the incident site, as illustrated in Fig. 3. Accordingly, X_b^σ should be the minimum spatial requirement to ensure that all these "$n_\sigma^{t_b}$" units of approaching AC vehicles of the targeted platoon stopping safely before

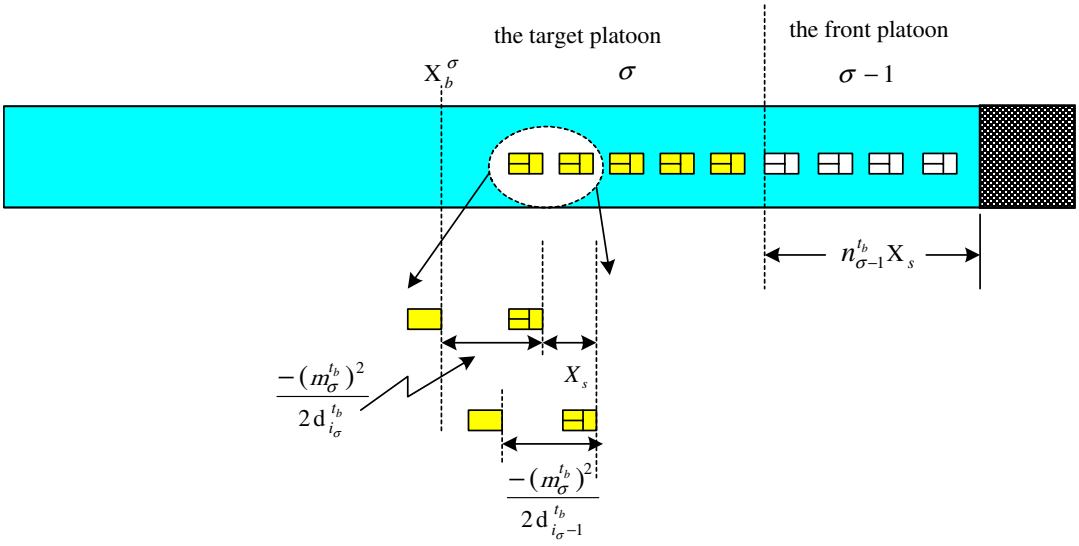

Fig. 3. Illustration of dynamic safety spacing for mandatory braking of AC vehicles.

hitting the tail of the last queued vehicle of the front platoon, $\sigma - 1$. Thus, we have the mathematical form of X_{b}^{σ} given by

$$X_{\mathrm{b}}^{\sigma} = \left[\sum_{i_\sigma=2}^{n_\sigma^{t_\mathrm{b}}} X_{\mathrm{s}} - \frac{(\mu_\sigma^{t_\mathrm{b}})^2}{2d_{i_\sigma}^{t_\mathrm{b}}} + \frac{(\mu_\sigma^{t_\mathrm{b}})^2}{2d_{i_\sigma-1}^{t_\mathrm{b}}}\right] + \left[X_{\mathrm{s}} - \frac{(\mu_\sigma^{t_\mathrm{b}})^2}{2d_1^{t_\mathrm{b}}}\right] + \left[n_{\sigma-1}^{t_\mathrm{b}} \times X_{\mathrm{s}}\right]$$
$$= \left[\sum_{i_\sigma=1}^{n_\sigma^{t_\mathrm{b}}} X_{\mathrm{s}} - \frac{(\mu_\sigma^{t_\mathrm{b}})^2}{2d_{i_\sigma}^{t_\mathrm{b}}}\right] + \left[\sum_{i_\sigma=2}^{n_\sigma^{t_\mathrm{b}}} \frac{(\mu_\sigma^{t_\mathrm{b}})^2}{2d_{i_\sigma-1}^{t_\mathrm{b}}}\right] + [n_{\sigma-1}^{t_\mathrm{b}} \times X_{\mathrm{s}}], \quad (1)$$

where X_{s} is the preset minimum vehicular spacing, from head to head, between any two adjoining AC vehicles of any given platoon queuing in the mandatory braking area; $d_{i_\sigma}^{t_\mathrm{b}}$ and $d_{i_\sigma-1}^{t_\mathrm{b}}$ represent the decelerations conducted by a given AC vehicle (i_σ) and its front vehicle ($i_\sigma - 1$) of the targeted platoon σ at time t_{b}, and both are negative values; and the head AC vehicle of the targeted platoon σ is represented by $i_\sigma = 1$. It is also noted that for convenience all the vehicular spacing variables specified in this study refer to the vehicular head-to-head measurements.

It is worth mentioning that the feasibility of Eq. (1) may depend highly on the postulated assumptions. In addition, two potential inter-vehicle spacing cases, i.e., equal-spacing and unequal-spacing, may warrant further discussion when these targeted AC vehicles are approaching the mandatory braking area. In the unequal-spacing scenario, the approaching AC vehicles should conduct braking maneuvers with different decelerations to maintain the static safety spacing after fully stopping for each pair of two sequential AC vehicles, and thus Eq. (1) can be directly employed to determine the time-varying threshold X_{b}^{σ}. Under the equal-spacing control condition corresponding to the condition that no AC vehicles conduct lane-changing maneuvers before reaching the mandatory braking zone, all the decelerations (denoted by $d_\sigma^{t_\mathrm{b}}$) associated with these approaching AC vehicles may stay the same. Accordingly, Eq. (1) can be simply rewritten as

$$X_{\mathrm{b}}^{\sigma} = n_\sigma^{t_\mathrm{b}} \times X_{\mathrm{s}} - \frac{(\mu_\sigma^{t_\mathrm{b}})}{2d_\sigma^{t_\mathrm{b}}} + n_{\sigma-1}^{t_\mathrm{b}} \times X_{\mathrm{s}}. \quad (2)$$

X_{f}^{σ} is specified to trigger the functionality of inter-vehicle spacing readjustment for these decomposed AC vehicles in response to the lane-blocking incident ahead. Herein, the area bounded between X_{f}^{σ} and X_{b}^{σ} is regarded as a buffer zone in which the dynamic spacing between any two decomposed AC vehicles of the target platoon σ is readjusted in preparation for conducting two potential automated-control maneuvers before they reach to the mandatory braking area: (1) car-following, and (2) incident-induced mandatory lane-changing. Given that right after being decomposed, the AC vehicles of the target platoon σ start to enter the aforementioned buffer area with the instantaneous platoon speed $\mu_\sigma^{t_\mathrm{f}}$ the same as the initial platoon speed $\mu_\sigma^{t_0}$ (i.e.,) and constant initial inter-vehicle spacing (i.e., $x_\sigma^{t_\mathrm{f}} = x_\sigma^{t_0}$) at time t_{f}, referring to the time that the first decomposed AC vehicle enters into this buffer zone. Then, the following two scenarios may occur sequentially.

First, the inter-vehicle spacing associated with any given pair of decomposed AC vehicles is enlarged in consideration of the safety factor in the car-following process. Such a mechanism is executed in sequence by each AC vehicle of the target platoon σ via deceleration maneuvers, starting from the rear AC vehicle. Thus, the phenomenon of deceleration propagation may form at this stage, and is followed by the stable condition that each AC vehicle keeps moving with a consistent speed and enlarged inter-vehicle spacing.

Second, to pass successfully by the incident site, some AC vehicles moving in the blocked lane upstream from the incident may conduct lane-changing maneuvers if the traffic flow conditions in adjacent lanes permit. At this moment, either acceleration or deceleration seems needed by lane-changing AC vehicles. Considering the basic requirement for safety in conducting the aforementioned two potential maneuvers, the initial disaggregate inter-vehicle spacing $x_\sigma^{t_\mathrm{f}}$ should then be adjusted as

$$x_\sigma^{t_\mathrm{f}} = \begin{cases} \left[\frac{A_{i_\sigma}^{\mathrm{mc}} \times (T_{\mathrm{mc}})^2}{2}\right] \times \cos(\Theta_{\mathrm{mc}}), & \text{if } \bar{v}_j^{t_\mathrm{f}} \geqslant u_\sigma^{t_\mathrm{f}} \\ \frac{(\bar{v}_j^{t_\mathrm{f}} - u_\sigma^{t_\mathrm{f}})^2}{2 \times D_{i_\sigma}^{\mathrm{mc}}}, & \text{otherwise,} \end{cases} \quad (3)$$

where $\bar{v}_j^{t_f}$ represents the average speed observed in the given adjacent lane j at time t_f; $A_{i_\sigma}^{mc}$ represents the preset maximum acceleration for the given AC vehicle i_σ to smoothly merge to the traffic flow of the given adjacent lane j in the process of mandatory lane changing (coded *mc* for short) under the condition that $\bar{v}_j^{t_f}$ is greater than $\mu_\sigma^{t_f}$; in contrast with $A_{i_\sigma}^{mc}$, $D_{i_\sigma}^{mc}$ refers to the corresponding maximum deceleration preset for the given AC vehicle i_σ, given that $\bar{v}_j^{t_f}$ is less than $\mu_\sigma^{t_f}$; T_{mc} refers to the average time spent to complete an incident-induced mandatory lane changing maneuver; Θ_{mc} is the preset turning angle allowable in the mandatory lane-changing process. It is noteworthy that in the above spacing control logic, we suggest that the speed of each decomposed AC vehicle be adjusted to be the same as the averaged speed of the adjacent lane at the beginning of the car-following zone, and then search for the lane-changing possibility in the incident-induced AC car-following procedure. Such a two-stage control mechanism may help to reach a new equilibrium condition of the link traffic flow as these AC vehicles are approaching to the incident site.

Accordingly, we can determine the dynamic threshold X_f^σ relative to the incident site, by

$$X_f^\sigma = X_b^\sigma + n_\sigma^{t_f} \times x_\sigma^{t_f}, \tag{4}$$

where $n_\sigma^{t_f}$ represents the number of the decomposed AC vehicles involved in the target platoon σ at time t_f. It is also worth mentioning that as some AC vehicles successfully complete lane-changing maneuvers within the buffer zone, the corresponding inter-vehicle gaps may turn out to be greater, leading to safer moving situations. Therefore, X_f^σ shown in Eq. (4) can be regarded as the minimum requirement for those AC vehicles moving in the car-following zone. For safety, it is also suggested that those AC vehicles of the target platoon σ remaining in the blocked lane maintain the same speed $u_\sigma^{t_f}$ until reaching the mandatory braking area, where $u_\sigma^{t_f} = \bar{v}_j^{t_f}$.

Threshold X_d^σ is derived to initialize the proposed incident-responsive AC vehicle control. In this scenario, the target high-speed AC platoon σ moving farther upstream from the incident site starts to decompose the corresponding linked AC vehicles once the head AC vehicle of the target platoon σ enters into the buffer area bounded by X_d^σ and X_f^σ. After the decomposition action, the AC control logic turns from centralization to be decentralization, whereby the disaggregated AC vehicles may take different traffic maneuvers in the process of approaching the incident site until they change lanes back to the blocked lane downstream from the incident site, reforming a new AC platoon. Herein, let us consider that there are $n_\sigma^{t_d}$ units of AC vehicles linked initially in the target platoon σ, moving with the same initial approaching speed $\mu_\sigma^{t_0}$ and static inter-vehicle spacing $x_\sigma^{t_0}$. Once the corresponding head AC vehicle enters the buffer area bounded by X_d^σ and X_f^σ at time t_d, the decentralization control mechanism of the target platoon σ will be triggered to conduct the disaggregated incident-responsive AC vehicle control, e.g., car-following, mandatory lane-changing, and braking, as described previously. Such a decomposition procedure is not completed until all the AC vehicles enter into this buffer area and move stably in preset buffer time T_d. Accordingly, we have

$$\begin{aligned} X_d^\sigma - X_f^\sigma &= \overline{L} + [(n_\sigma^{t_d} - 1) \times (\overline{L} + x_\sigma^{t_0})] + u_\sigma^{t_0} \times T_d \Rightarrow X_d^\sigma \\ &= X_f^\sigma + \{\overline{L} + [(n_\sigma^{t_d} - 1) \times (\overline{L} + x_\sigma^{t_0})] + u_\sigma^{t_0} \times T_d\}, \end{aligned} \tag{5}$$

where $\overline{L}$ represents the preset average vehicular length in the system.

4. Lane-changing maneuvers

The automated lane-changing control logic is herein proposed to deal with lane-changing maneuvers of the disaggregated AC vehicles in the presence of a lane-blocking incident ahead. Such incident-induced mandatory lane-changing behavior is required for each AC vehicle, and must be conducted in the processes of both approaching to the incident site from the blocked lane, and lane-changing-back from a given adjacent lane to the blocked lane, after passing by the incident site, to re-form a new AC platoon. Accordingly, three sequential phases, including: (1) mandatory lane-changing upstream from the blocked AC lane to the corresponding adjacent lane, (2) mix-flow car following, and (3) return-lane-changing from the adjacent lane to the AC lane downstream to the incident site, are involved in the proposed control logic, as illustrated in Fig. 4. The corresponding microscopic control models are presented below.

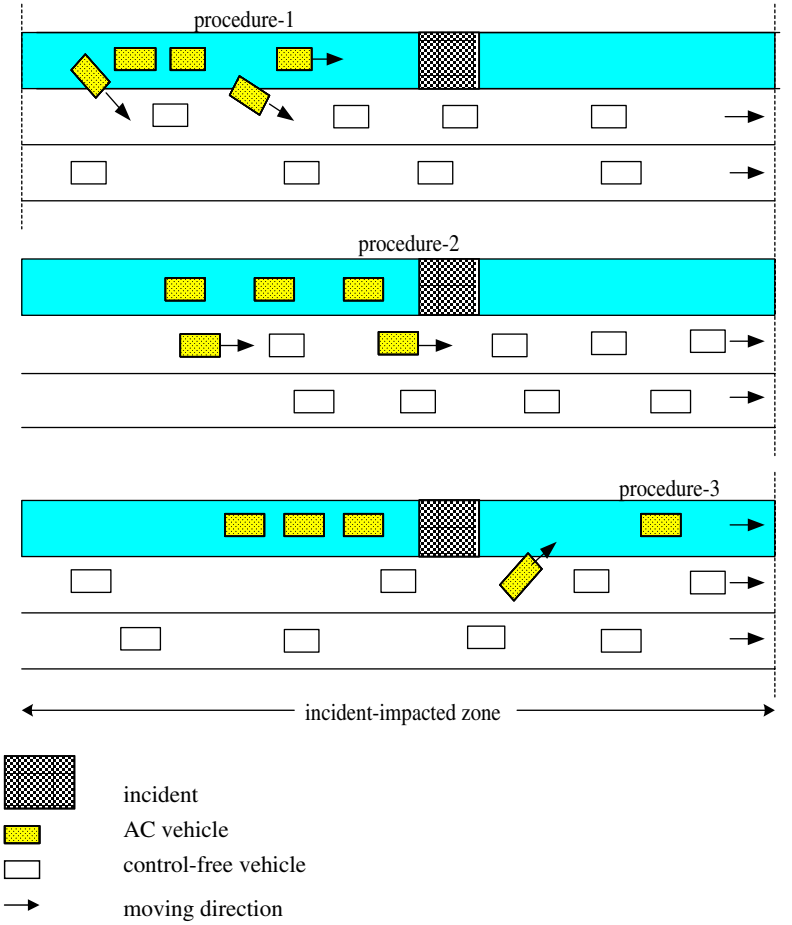

Fig. 4. Scenarios of incident-induced mandatory lane-changing maneuvers in AHS AC vehicle i_σ potentially conducting lane-changing behaviour at time t.

4.1. Upstream mandatory lane-changing modeling

The control logic proposed in this scenario aims to regulate the incident-induced mandatory lane-changing maneuvers of AC vehicles while they are moving in either the car-following buffer zone or the mandatory braking zone, after the target AC platoon is decomposed. Compared to our previous research (Sheu et al., 2001; Sheu and Ritchie, 2001), which aimed at modeling incident-induced mandatory lane-changing behavior in the fully manual-control traffic environment, the challenging issue remaining at this point is how to make appropriate decisions that permit these AC vehicles to safely merge into the manual-control traffic flows under the condition of a lane-blocking incident. To simplify the corresponding problem formulation, the incident effect on the traffic in the adjacent lane is not considered in the current study, although the aforementioned hypothesis may not hold in some cases. Herein, the proposed lane-changing control logic deals with the upstream mandatory lane-changing behavior via two sequential stages, including (1) pre-action decision-making and (2) in-action lane-changing operations. The corresponding control logic models are detailed below.

4.1.1. Stage 1: Pre-action decision-making

The decision-making model proposed in this stage aims to determine if an action of mandatory lane changing is permitted under the present traffic flow conditions of the target adjacent lane, referring to the given adjacent lane that a given AC vehicle is preparing to enter using lane-changing behavior. In this

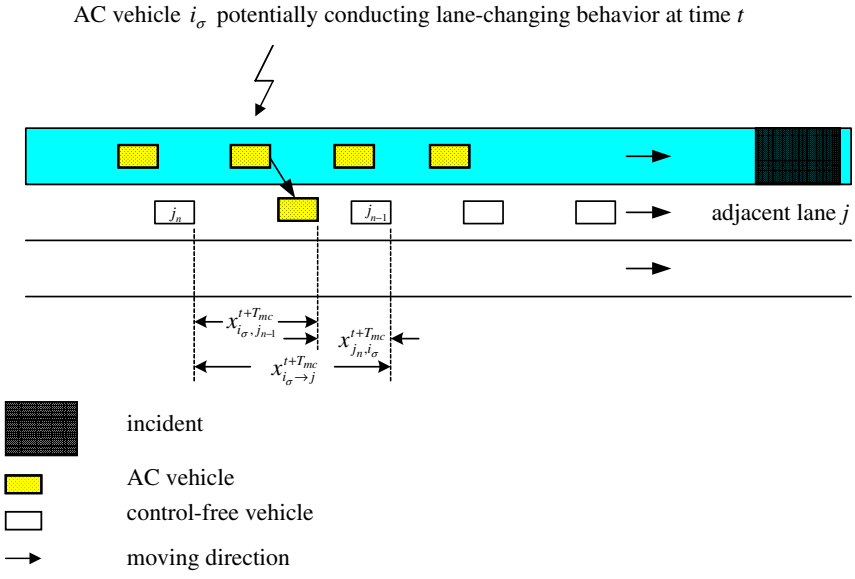

Fig. 5. The adjacent-lane dynamic spacing for consideration of lane changing.

scenario, the potential change of dynamic spacing in the adjacent lane is regarded as the major factor influencing the decision-making of mandatory lane changing. The corresponding three conditions are derived below.

First, let us consider the dynamic spacing of the adjacent lane, which includes three elements, i.e., $x_{i_\sigma\to j}^{t+T_{\mathrm{mc}}}$, $x_{i_\sigma,j_{n-1}}^{t+T_{\mathrm{mc}}}$ and $x_{j_n,i_\sigma}^{t+T_{\mathrm{mc}}}$. As can be seen in Fig. 5, $x_{i_\sigma\to j}^{t+T_{\mathrm{mc}}}$ refers to the forecasted post-action vehicular head-to-head dynamic spacing bounded by two vehicles present in the adjacent lane j, i.e., j_n and j_{n-1}, given that the corresponding mandatory lane-changing behavior associated with the given AC vehicle i_σ is considered at time t, and expected to be completed at time $t + T_{\mathrm{mc}}$. Herein, $x_{i_\sigma\to j}^{t+T_{\mathrm{mc}}}$ can be further decomposed into two elements: (1) $x_{i_\sigma,j_{n-1}}^{t+T_{\mathrm{mc}}}$, which refers to the adjusted inter-vehicle head-to-head spacing both between j_{n-1} and i_σ $(x_{i_\sigma,j_{n-1}}^{t+T_{\mathrm{mc}}})$; and (2) $x_{j_n,i_\sigma}^{t+T_{\mathrm{mc}}}$, which represents the corresponding dynamic spacing between i_σ and j_n. According to our control logic, the given AC vehicle i_σ may conduct the mandatory lane-changing behavior only when the following three critical conditions simultaneously hold.

4.1.1.1. Condition 1. The forecasted post-action spacing $(x_{i_\sigma\to j}^{t+T_{\mathrm{mc}}})$ must be greater than the present corresponding spacing of the adjacent lane faced by the given AC vehicle $i_\sigma(x_{i_\sigma\to j}^{t})$ observed at time t, as expressed mathematically in Eq. (6)

$$x_{i_\sigma\to j}^{t+T_{\mathrm{mc}}} > x_{i_\sigma\to j}^{t} \Rightarrow x_{i_\sigma\to j}^{t+T_{\mathrm{mc}}} > X_{j_n}^{t} - X_{j_{n-1}}^{t}, \tag{6}$$

where $X_{j_n}^{t}$ and $X_{j_n-1}^{t}$ represent the time-varying longitudinal locations of the corresponding adjacent-lane vehicles j_n and j_{n-1}, relative to the incident site at time t, respectively. Herein, $x_{i_\sigma\to j}^{t+T_{\mathrm{mc}}}$ can be regarded as the inference drawn from a sequence of the speed-adjustment maneuvers between the given AC vehicle i_σ and the adjacent-lane vehicles, including j_n and j_{n-1}, in the lane-changing process of the given AC vehicle i_σ. For safety concerns, let us consider the following critical case in which the downstream vehicle of the adjacent lane j_{n-1} with the initial speed $v_{j_{n-1}}^{t}$ may decelerate with the maximum deceleration $D_{j_{n-1}}^{t}$ at time t in response to the farther downstream traffic flow conditions in the lane-changing process of i_σ, and meanwhile the upstream vehicle j_n with the initial speed $v_{j_n}^{t}$ may decelerate with any potential deceleration $d_{j_\eta}^{t}$ in response to the merged AC vehicle i_σ from the blocked automated-lane i, which is characterized by the initial speed $u_{i_\sigma}^{t}$, predetermined maximum allowable acceleration $A_{i_\sigma}^{\mathrm{mc}}$, safety turning angle Θ_{mc} and time spent in lane chang-

ing T_{mc}. Following the aforementioned two-stage speed-adjustment postulation, we then have the adjusted inter-vehicle head-to-head spacing both between j_{n-1} and $i_\sigma(x_{i_\sigma,j_{n-1}}^{t+T_{mc}})$, and between i_σ and $j_n(x_{j_n,i_\sigma}^{t+T_{mc}})$ derived respectively by

$$\begin{aligned} x_{i_\sigma,j_{n-1}}^{t+T_{mc}} &= X_{i_\sigma}^{t+T_{mc}} - X_{j_{n-1}}^{t+T_{mc}} \\ &= \left\{ X_{i_\sigma}^{t} - \left[u_{i_\sigma}^{t} \times T_{mc} + \frac{1}{2} \times A_{i_\sigma}^{mc} \times (T_{mc})^2 \right] \times \cos(\Theta_{mc}) \right\} - \left[X_{j_{n-1}}^{t} - v_{j_{n-1}}^{t} \times T_{mc} - \frac{1}{2} D_{j_{n-1}}^{t} \times (T_{mc})^2 \right], \end{aligned} \tag{7}$$

$$\begin{aligned} x_{j_n,i_\sigma}^{t+T_{mc}} &= X_{j_n}^{t+T_{mc}} - X_{i_\sigma}^{t+T_{mc}} \\ &= \left[X_{j_n}^{t} - v_{j_n}^{t} \times T_{mc} - \frac{1}{2} \times d_{j_n}^{t} \times (T_{mc})^2 \right] - \left\{ X_{i_\sigma}^{t} - \left[u_{i_\sigma}^{t} \times T_{mc} + \frac{1}{2} \times A_{i_\sigma}^{mc} \times (T_{mc})^2 \right] \times \cos(\Theta_{mc}) \right\}, \end{aligned} \tag{8}$$

where $X_{j_n}^{t+T_{mc}}$ and $X_{j_n-1}^{t+T_{mc}}$ represent the time-varying longitudinal locations of the corresponding adjacent-lane vehicles j_n and j_{n-1}, relative to the incident site at time $t + T_{mc}$; and similarly, $X_{i_\sigma}^{t+T_{mc}}$ represents the time-varying longitudinal location of the given AC vehicle i_σ, relative to the incident site at time $t + T_{mc}$. Considering Eqs. (7) and (8), the aforementioned lane-changing permission condition shown in Eq. (6) can then be rewritten as

$$\left[v_{j_{n-1}}^{t} \times T_{mc} + \frac{1}{2} \times D_{j_{n-1}}^{t} \times (T_{mc})^2 \right] - \left[v_{j_n}^{t} \times T_{mc} + \frac{1}{2} \times d_{j_n}^{t} \times (T_{mc})^2 \right] > 0, \tag{9}$$

where $d_{j_n}^{t}$ and $D_{j_{n-1}}^{t}$ are negative values. Nevertheless, in some cases, the upstream adjacent-lane vehicle j_n may keep moving without any attempts of deceleration at time t. Due to safety concerns, Eq. (10) is derived particularly for this demanding condition.

$$\left[v_{j_{n-1}}^{t} \times T_{mc} + \frac{1}{2} \times D_{j_{n-1}}^{t} \times (T_{mc})^2 \right] - (v_{j_n}^{t} \times T_{mc}) > 0. \tag{10}$$

4.1.1.2. Condition 2. The forecasted post-action spacing between j_{n-1} and $i_\sigma(x_{i_\sigma,j_{n-1}}^{t+T_{mc}})$ must be greater than the dynamic length of the vehicle moving in front of the given AC vehicle i_σ, as expressed in Eq. (11).

$$x_{i_\sigma,j_{n-1}}^{t+T_{mc}} > (1+\varphi) \times \overline{L} + u_{i_\sigma}^{t+T_{mc}} \times \tau. \tag{11}$$

The right hand side of Eq. (11) refers to the dynamic length of the corresponding front vehicle perceived by the given AC vehicle i_σ, where $u_{i_\sigma}^{t+T_{mc}}$ represents the post-action speed of the given AC vehicle i_σ after completing lane-changing behavior at time $t + T_{mc}$; τ refers to the predetermined buffer time associated with any given AC vehicle in response to the changes of vehicular speed ahead; and φ represents the preset static safety spacing measured from the tail of the front vehicle $(j_n - 1)$ to the head of the given AC vehicle (i_σ), and herein φ is preset to be a value of 0.1. Note that the concept of vehicular dynamic length was employed in our previous research (Chou and Sheu, 1992) to specify the dynamic thresholds of inter-vehicle safety spacing. Therein, we suggested that the minimum requirement of the head-to-head spatial gap kept between any two adjacent vehicles moving in a given lane should be dynamic, and proportional to the running speed and corresponding reaction time of the rear vehicle. Such a minimum gap requirement corresponds to the dynamic length of the front vehicle perceived by the corresponding rear vehicle. It is also worth mentioning that although the rear vehicle in this scenario refers to an AC vehicle, the concept of the reaction time may be still applicable to the case in which the given AC vehicle is moving with other control-free vehicles in a given lane.

Combining Eq. (7) with Eq. (11), Condition 2 can then be rewritten as

$$\begin{aligned}
&\left\{X^t_{i_\sigma} - \left[u^t_{i_\sigma} \times T_{\mathrm{mc}} + \frac{1}{2} \times A^{\mathrm{mc}}_{i_\sigma} \times (T_{\mathrm{mc}})^2\right] \times \cos(\Theta_{\mathrm{mc}})\right\} \\
&\quad - \left[X^t_{j_{n-1}} - v^t_{j_{n-1}} \times T_{\mathrm{mc}} - \frac{1}{2} D^t_{j_{n-1}} \times (T_{\mathrm{mc}})^2\right] > (1+\varphi) \times \overline{L} + u^{t+T_{\mathrm{mc}}}_{i_\sigma} \times \tau \\
&\quad \Rightarrow \left\{X^t_{i_\sigma} - \left[u^t_{i_\sigma} \times (T_{\mathrm{mc}} + \tau) + A^{\mathrm{mc}}_{i_\sigma} \times T_{\mathrm{mc}} \times \left(\frac{1}{2} \times T_{\mathrm{mc}} + \tau\right)\right] \times \cos(\Theta_{\mathrm{mc}})\right\} \\
&\quad - \left[X^t_{j_{n-1}} - v^t_{j_{n-1}} \times T_{\mathrm{mc}} - \frac{1}{2} D^t_{j_{n-1}} \times (T_{\mathrm{mc}})^2\right] - (1+\varphi) \times \overline{L} > 0. \qquad (12)
\end{aligned}$$

4.1.1.3. Condition 3. The forecasted post-action spacing between i_σ and $j_n(x^{t+T_{\mathrm{mc}}}_{j_n,j_\sigma})$ must be greater than the dynamic length of the moving AC vehicle perceived by j_n. Similarly, employing the aforementioned concept of dynamic vehicular length together with Eq. (8), Condition 3 can then be derived as follows.

$$\begin{aligned}
&x^{t+T_{\mathrm{mc}}}_{j_n,i_\sigma} > (1+\varphi) \times \overline{L} + v^{t+T_{\mathrm{mc}}}_{j_n} \times \tau \\
&\quad \Rightarrow \left[X^t_{j_n} - v^t_{j_n} \times (T_{\mathrm{mc}} + \tau) - d^t_{j_n} \times T_{\mathrm{mc}} \times \left(\frac{1}{2} \times T_{\mathrm{mc}} + \tau\right)\right] \\
&\qquad - \left\{X^t_{i_\sigma} - \left[u^t_{i_\sigma} \times T_{\mathrm{mc}} + \frac{1}{2} \times A^{\mathrm{mc}}_{i_\sigma} \times (T_{\mathrm{mc}})^2\right] \times \cos(\Theta_{\mathrm{mc}})\right\} - (1+\varphi) \times \overline{L} > 0. \qquad (13)
\end{aligned}$$

Note that in most of the above equations, we suggest using the boundary values (e.g., $A^{\mathrm{mc}}_{i_\sigma}$ and $D^t_{j_{n-1}}$) to derive the most demanding conditions used for pre-action decision making of lane changing. In reality, such a treatment is highly recommended in our study since due to the concerns of safety and efficiency in calculation in the corresponding decision making process.

4.1.2. Stage 2: In-action lane-changing operations

This scenario aims to determine control variables of the mandatory lane-changing maneuver associated with the given AC vehicle i_σ, given the decision made in the previous stage indicating that the corresponding lane-changing maneuver is allowed at this moment. Compared to the previous decision, which determines whether or not the mandatory lane-changing behavior is permitted, the control variables determined in this phase serve to help any given AC vehicle to merge safely and smoothly into the adjacent-lane traffic flow under various traffic flow conditions in adjacent lanes. Accordingly, to determine if the incident-induced mandatory lane-changing maneuver of the given AC vehicle i_σ can be completed successfully in the unit time interval T_{mc}, we investigate two corresponding time-varying control variables used in the proposed lane-changing control logic, including: (1) the time-varying turning angle ($\theta^t_{i_\sigma}$), and (2) the speed adjustment rate ($\alpha^t_{i_\sigma}$). The derivations of these control variables are described below.

The determination of the time-varying turning angle ($\theta^t_{i_\sigma}$) primarily considers the following two factors: (1) the potential conflict points between the given AC vehicle i_σ and the front AC vehicle $i_\sigma - 1$ moving ahead, as illustrated in Fig. 6; and (2) the dynamic safety spacing relative to the front control-free vehicle of the adjacent lane j (i.e., j_{n-1}), in the process of lane changing. Correspondingly, the following two conditions, i.e., Eqs. (14) and (15), must hold to determine $\theta^t_{i_\sigma}$.

$$\theta^t_{i_\sigma} > \vec{\theta}^t_{i_\sigma} \qquad (14)$$

$$\begin{aligned}
&\left\{X^t_{i_\sigma} - \left[u^t_{i_\sigma} \times (T_{\mathrm{mc}} + \tau) + \alpha^t_{i_\sigma} \times T_{\mathrm{mc}} \times \left(\frac{1}{2} \times T_{\mathrm{mc}} + \tau\right)\right] \times \cos(\theta^t_{i_\sigma})\right\} \\
&\quad - \left[X^t_{j_{n-1}} - v^t_{j_{n-1}} \times T_{\mathrm{mc}} - \frac{1}{2} D^t_{j_{n-1}} \times (T_{\mathrm{mc}})^2\right] - (1+\varphi) \times \overline{L} > 0, \qquad (15)
\end{aligned}$$

where

$$\vec{\theta}^t_{i_\sigma} = \tan^{-1}\left\{\frac{\overline{W}}{X^t_{i_\sigma} - X^t_{i_\sigma - 1} - \overline{L}}\right\} \qquad (16)$$

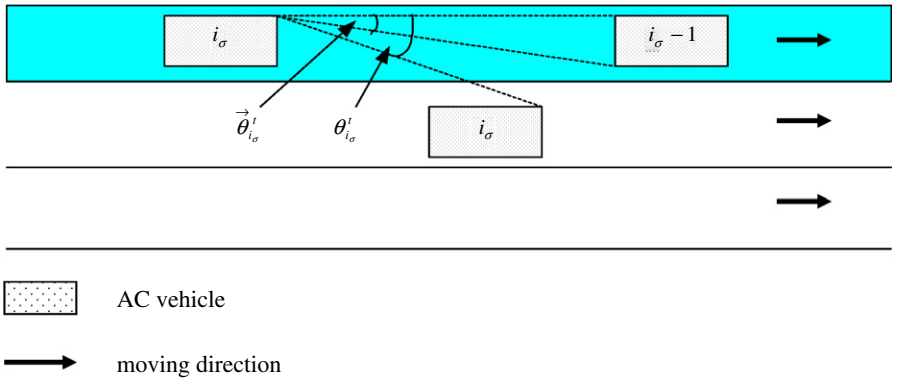

Fig. 6. Illustration of the time-varying turning angle.

and $\overline{W}$ represents the predetermined average vehicular width. Apparently, Eq. (15) is a form of Eq. (12) revised by replacing both Θ_{mc} and $A^{\mathrm{mc}}_{i_\sigma}$ with $\theta^t_{i_\sigma}$ and $\alpha^t_{i_\sigma}$, respectively. Now, according to Eq. (14), let the tentative value of $\theta^t_{i_\sigma}$ (i.e., $\tilde{\theta}^t_{i_\sigma}$) be

$$\tilde{\theta}^t_{i_\sigma} = \tan^{-1}\left\{\frac{\overline{W} + X^w_{\mathrm{s}}}{X^t_{i_\sigma} - X^t_{i_\sigma - 1} - \overline{L}}\right\}, \tag{17}$$

where X^w_{s} represents the static lateral safety spacing predetermined in this study. Combining Eqs. (15) and (17), i.e., by replacing $\theta^t_{i_\sigma}$ with $\tilde{\theta}^t_{i_\sigma}$ in Eq. (15), then the instantaneous turning angle $\theta^t_{i_\sigma}$ can be determined by

$$\theta^t_{i_\sigma} = \begin{cases} \tilde{\theta}^t_{i_\sigma}, & \text{if Eq. (15) holds true} \\ \Theta_{\mathrm{mc}}, & \text{otherwise.} \end{cases} \tag{18}$$

The speed adjustment serves to regulate the speed of the given lane-changing AC vehicle i_σ to be consistent with the corresponding front vehicle of the adjacent lane j_{n-1} in the given lane-changing time interval T_{mc}. Correspondingly, the following basic condition must hold:

$$v^t_{j_{n-1}} = (u^t_{i_\sigma} + \alpha^t_{i_\sigma} \times T_{\mathrm{mc}}) \times \cos(\theta^t_{i_\sigma}), \tag{19}$$

where $\theta^t_{i_\sigma}$ refers to the time-varying turning angle determined in the previous phase. However, the speed adjustment procedure must also consider the corresponding upper bound, i.e., $A^{\mathrm{mc}}_{i_\sigma}$ and $D^{\mathrm{mc}}_{i_\sigma}$ for acceleration and deceleration cases, respectively. Therefore, we have the time-varying speed adjustment rate $\alpha^t_{i_\sigma}$ finalized as

$$\alpha^t_{i_\sigma} = \begin{cases} \min\left[\frac{v^t_{j_n-1} - u^t_{i_\sigma} \times \cos(\theta^t_{i_\sigma})}{T_{\mathrm{mc}} \times \cos(\theta^t_{i_\sigma})}, A^t_{i_\sigma}\right], & \text{if } v^t_{j_{n-1}} \geqslant u^t_{i_\sigma} \times \cos(\theta^t_{i_\beta}) \\ \max\left[\frac{v^t_{j_n-1} - u^t_{i_\sigma} \times \cos(\theta^t_{i_\sigma})}{T_{\mathrm{mc}} \times \cos(\theta^t_{i_\sigma})}, D^t_{i_\sigma}\right], & \text{otherwise.} \end{cases} \tag{20}$$

4.2. Mixed-flow car-following modeling

The control logic proposed here aims to regulate each merged AC vehicle to move smoothly and safely into the given adjacent lane j with other manually-driven vehicles until passing by the incident site. Note that given automated and manual traffic mixed in the non-automated lane, the reaction of any given manually-driven vehicle to the corresponding front vehicle is supposed to follow general car-following maneuvers, which can be characterized by the existing car-following models, and thus is not addressed in this subsection. Compared to environments described by other existing car-following models, the intra-lane traffic flow environments existing in this scenario are more complicated for the following two reasons. First, any given AC

vehicle must respond dynamically and automatically to its front vehicle no matter whether or not the corresponding front vehicle is of automated control. Correspondingly, the stimulus source coming from the corresponding front vehicle may be driven by human factors because of its manual control; however, the stimulus respondence, i.e., the given AC vehicle, should be of automated control without the need of human factors. Second, the existing traffic flow of the given adjacent lane j moving upstream from the incident site, including any merged AC vehicles, may also be affected by the incident impact due to any upcoming lane-changing AC vehicles in the following time intervals, and the driver's hesitation at any front manual-control vehicles while passing by the incident site. Therefore, a specific mixed-flow car-following control model is derived as follows.

According to the aforementioned goal of the proposed control logic and corresponding distinctive features of this scenario, we further consider three critical factors involved in the proposed mix-flow car-following control model: (1) the dynamic length of the corresponding front vehicle perceived by the given AC vehicle i_σ in the given adjacent lane after completing lane changing, (2) the instantaneous speed of the corresponding front vehicle $j_n - 1$, and (3) the instantaneous aggregated speed of the adjoining platoon in front of i_σ. Note that the involvement of the first factor, i.e., the dynamic length of the front vehicle is to satisfy the basic safety requirement in terms of vehicular spacing when any given AC vehicle moving in the mix traffic flow environment; in contrast, consideration of the other two factors is to alleviate the incident-induced lane traffic disturbance in front of the given AC vehicle, and correspondingly make the given AC vehicle move smoothly without the need to conduct any unusual speed adjustment. Accordingly, we propose a dynamic mix-flow car-following model used to determine the time-varying speed adjustment rate associated with the given AC vehicle i_σ at given time $t_{\mathrm{mc}}(\alpha_{i_\sigma}^{t_{\mathrm{mc}}})$ as

$$\alpha_{i_\sigma}^{t_{\mathrm{mc}}} = w_1^{t_{\mathrm{mc}}} \times \frac{(v_{j_n-1}^{t_{\mathrm{mc}}})^2 - (u_{i_\sigma}^{t_{\mathrm{mc}}})^2}{2[X_{i_\sigma}^{t_{\mathrm{mc}}} - X_{j_n-1}^{t_{\mathrm{mc}}} - ((1+\varphi)\times \overline{L} + u_{i_\sigma}^{t_{\mathrm{mc}}} \times \tau)]} + w_2^{t_{\mathrm{mc}}} \times \left[\frac{\overline{V}_{\mathrm{P}_{n-1}}^{t_{\mathrm{mc}}} - u_{i_\sigma}^{t_{\mathrm{mc}}}}{\tau}\right], \tag{21}$$

where $u_{i_\sigma}^{t_{\mathrm{mc}}}$ and $v_{j_n-1}^{t_{\mathrm{mc}}}$ represent the instantaneous speeds of the given AC vehicle i_σ and the corresponding front vehicle $(j_n - 1)$ in the adjacent lane observed at time t_{mc} given $t_{\mathrm{mc}} \geqslant t + T_{\mathrm{mc}}$; similarly, $X_{i_\sigma}^{t_{\mathrm{mc}}}$ and $X_{j_n-1}^{t_{\mathrm{mc}}}$ refer to the instantaneous longitudinal locations of the given AC vehicle i_σ and the corresponding front vehicle $j_n - 1$ in the adjacent lane j observed at time t_{mc}, relative to the incident site; $\overline{V}_{\mathrm{P}_{n-1}}^{t_{\mathrm{mc}}}$ represents the instantaneous aggregate speed of the adjoining platoon (P_{n-1}) present in front of vehicle i_σ at time t_{mc}; both $w_1^{t_{\mathrm{mc}}}$ and $w_2^{t_{\mathrm{mc}}}$ are dynamic weights indicating the incident effect on the corresponding speed adjustments at time t_{mc}. The potential spatial relationships among the vehicles i_σ, $j_n - 1$, and the adjoining platoon (P_{n-1}) are illustrated in Fig.7. Here, we assume that $w_1^{t_{\mathrm{mc}}}$ and $w_2^{t_{\mathrm{mc}}}$ follow negative exponential functions, depending on the time-varying distances of the corresponding leading vehicles, relative to the incident site. In addition, we also take account of the dynamic spacing $(X_{\mathrm{P}_{n-1}\to i_\sigma}^{t_{\mathrm{mc}}})$ between the corresponding leading vehicle of the front platoon P_{n-1} and the given AC vehicle i_σ in modeling the corresponding function of $w_2^{t_{\mathrm{mc}}}$ to reflect the magnitude of the

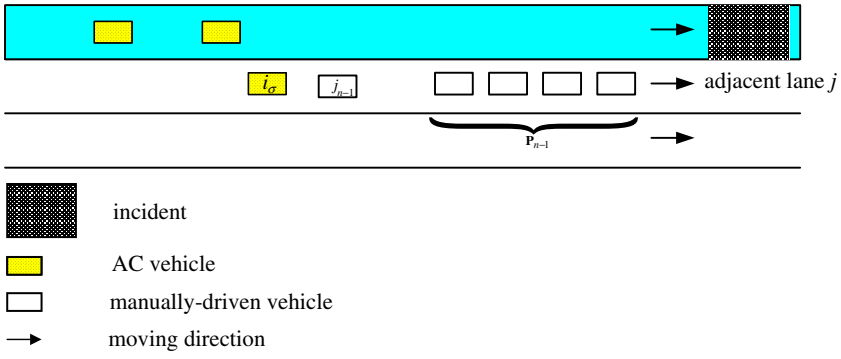

Fig. 7. Illustration of the spatial relationships among vehicles i_σ, $j_n - 1$, and platoon P_{n-1}.

influence oriented from the front platoon in the process of corresponding speed adjustment of i_σ. The mathematical forms of $w_1^{t_{mc}}$ and $w_2^{t_{mc}}$ are given respectively by

$$w_1^{t_{mc}} = \frac{e^{-X_{j_n-1}^{t_{mc}}}}{e^{-X_{j_n-1}^{t_{mc}}} + e^{-\left(X_{P_{n-1}}^{t_{mc}} + X_{P_{n-1}\to i_\sigma}^{t_{mc}}\right)}}, \tag{22}$$

$$w_2^{t_{mc}} = \frac{e^{-\left(X_{P_{n-1}}^{t_{mc}} + X_{P_{n-1}\to i_\sigma}^{t_{mc}}\right)}}{e^{-X_{j_n-1}^{t_{mc}}} + e^{-\left(X_{P_{n-1}}^{t_{mc}} + X_{P_{n-1}\to i_\sigma}^{t_{mc}}\right)}}, \tag{23}$$

where $X_{P_{n-1}}^{t_{mc}}$ represents the instantaneous longitudinal location associated with the leading vehicle of the front platoon (P_{n-1}) observed at time t_{mc}, relative to the incident site; and similarly $X_{P_{n-1}\to i_\sigma}^{t_{mc}}$ represents the dynamic spacing between the given AC vehicle i_σ and the corresponding leading vehicle of the front platoon P_{n-1} observed at time t_{mc}.

The rationale of the proposed mix-flow car-following model mentioned above is discussed below in several aspects. First, according to our previous research experiences (Sheu et al., 2001; Sheu, 2002 and 2003), in the presence of a lane-blocking incident, any given vehicle approaching the incident site may adjust its speed based not only on the front vehicle but also on the front platoon which is also approaching the incident. Such an argument relies on the hypothesis that under conditions of lane-blocking incidents, any given vehicle tends to coordinate its speed with the aggregate speed of the incident-impacted traffic platoon moving ahead in response to incident effects on intra-lane traffic flows. Therefore, the corresponding factor in terms of the instantaneous aggregate speed of the front adjoining platoon is involved, as shown in the second item of Eq. (21), to formulate the proposed incident-induced car-following model. Second, it seems agreeable that the closer any given vehicle approaches the incident site, the more significant the incident effect on the corresponding vehicular speed is, and vice versa. Accordingly, we add the corresponding time-varying weights associated with these two speed adjustment sources, i.e., the front vehicle and adjoining platoon, as shown in Eqs. (22) and (23), to indicate the corresponding incident effects on the speed adjustment of the given AC vehicle.

In addition, we illustrate the following several significant phases which potentially exist in the mix-flow car-following scenario, for further discussions.

Case 1. The front vehicle $j_n - 1$ belongs to the front platoon P_{n-1}, which is approaching upstream to the incident site. This is a typical case for which the proposed model shown in Eq. (21) can be directly applied. Clearly, the given AC vehicle i_σ may adjust its speed in response to both the average speed of P_{n-1} and the instantaneous speed of $j_n - 1$, i.e., the rear vehicle of P_{n-1}, with different degrees, according to our proposed model.

Case 2. Both the given AC vehicle i_σ and the front vehicle $j_n - 1$ are far from P_{n-1}, which is however relatively close to the incident site, compared to both i_σ and $j_n - 1$. This is another typical case which illustrates the distinctive feature of the proposed model. One corresponding condition is that $w_1^{t_{mc}} = w_2^{t_{mc}} = \frac{1}{2}$, under which the proposed model, Eq. (21), may turn out to be

$$\alpha_{i_\sigma}^{t_{mc}} = \frac{1}{2} \times \left\{ \frac{\left(v_{j_n-1}^{t_{mc}}\right)^2 - \left(u_{i_\sigma}^{t_{mc}}\right)^2}{2[X_{i_\sigma}^{t_{mc}} - X_{j_n-1}^{t_{mc}} - ((1+\varphi)\times \overline{L} + u_{i_\sigma}^{t_{mc}} \times \tau)]} + \left[\frac{\overline{V}_{P_{n-1}}^{t_{mc}} - u_{i_\sigma}^{t_{mc}}}{\tau} \right] \right\}. \tag{24}$$

Right after this moment, the corresponding effect resulting from the front platoon will lessen, as the platoon gradually leaves the incident site.

Case 3. There is only one vehicle ($j_n - 1$) in front of i_σ, before they pass by the incident site, and meanwhile $j_n - 1$ is significantly far from P_{n-1} which is presented downstream from the incident site. This case appears to diminish the effect of speed adjustment oriented from the second term of Eq. (21). Therefore, the weight $w_2^{t_{mc}}$ turns out to be rather slight, compared to $w_1^{t_{mc}}$. Accordingly, if we further assume that $w_2^{t_{mc}}$ is ignored, which will lead the proposed model to

$$\alpha_{i_\sigma}^{t_{mc}} = \frac{\left(v_{j_n-1}^{t_{mc}}\right)^2 - \left(u_{i_\sigma}^{t_{mc}}\right)^2}{2[X_{i_\sigma}^{t_{mc}} - X_{j_n-1}^{t_{mc}} - ((1+\varphi)\times \overline{L} + u_{i_\sigma}^{t_{mc}} \times \tau)]}. \tag{25}$$

Herein, the speed adjustment condition exhibited by Eq. (25) mimics the incident-free car-following behavior. That is, in this scenario the movement of the given AC vehicle i_σ is only influenced by the front vehicle $j_n - 1$.

Case 4. The time-varying speed of the given AC vehicle i_σ is consistent with that of the front vehicle $j_n - 1$ at time t_{mc}, i.e., $u_{i_\sigma}^{t_{\mathrm{mc}}} = v_{j_n-1}^{t_{\mathrm{mc}}}$. In this case, the given AC vehicle i_σ may still adjust its speed to earlier respond to the traffic condition further ahead, while it is approaching to the incident site. According to our proposed model, the corresponding speed adjustment rate ($\alpha_{i_\sigma}^{t_{\mathrm{mc}}}$) then turns out to be

$$\alpha_{i_\sigma}^{t_{\mathrm{mc}}} = w_2^{t_{\mathrm{mc}}} \times \frac{\overline{V}_{\mathrm{P}_{n-1}}^{t_{\mathrm{mc}}} - u_{i_\sigma}^{t_{\mathrm{mc}}}}{\tau}. \tag{26}$$

It is worth mentioning that the proposed incident-induced mix-flow car-following model is employed to deal with the movement of any given AC vehicle, which is approaching to the incident site via the adjacent lane, until it passes by the incident site. Right after this, the return-lane-changing behavior is considered to resume another AC platoon moving in the automated lane downstream from the incident site.

4.3. Return-lane-changing modeling

After passing by the incident site from the adjacent control-free lane, any given AC vehicle performs lane-changing behavior with the proposed return-lane-changing control logic to reform the platoon. To simplify return-lane-changing maneuvers of AC vehicles under control, two corresponding principles are postulated for the control logic. First, those AC vehicles passing by the incident site are coordinated to conduct return lane changes in sequence starting from the farthest upstream AC vehicle in the adjacent control-free lane. Second, the aforementioned multi-vehicle return-lane-changing mechanism is executed at each preset time interval π until all the approaching AC vehicles upstream from the incident site return to the AC lane after passing by the incident site. Compared to mandatory lane-changing described previously, the factors considered in the proposed return-lane-changing logic are relatively simple because the influence factors resulting from the corresponding rear vehicle in the AC lane no longer exist in the process of return-lane-changing procedure. In addition, the traffic characteristics, e.g., running speed and instantaneous speed adjustment exhibited by any AC vehicles presented upstream in the AC lane are under control. Accordingly, any AC vehicle can readily conduct such discretionary lane-changing behavior obeying the following operational conditions embedded in the proposed control logic rules,

$$\alpha_{i_\sigma}^{t_{\mathrm{rc}}} = \frac{u_\sigma^{t_0} - u_{i_\sigma}^{t_{\mathrm{rc}}} \times \cos(\Theta_{\mathrm{rc}})}{T_{\mathrm{rc}} \times \cos(\Theta_{\mathrm{rc}})}, \tag{27}$$

where $\alpha_{i_\sigma}^{t_{\mathrm{rc}}}$ represents the instantaneous speed adjustment rate associated with the given AC vehicle i_σ conducted at time t_{rc} in the return-lane-changing process (*rc* for short); $u_\sigma^{t_0}$, as described above, is the initial platoon speed predetermined in the AC system; $u_{i_\sigma}^{t_{\mathrm{rc}}}$ refers to the instantaneous speed of i_σ observed at time t_{rc}; similar to T_{mc}, T_{rc} represents the preset time spent in return-lane-changing for each given AC vehicle; Θ_{rc} is the turning angle preset for each AC vehicle in the return-lane-changing process.

Accordingly, the following transitional condition may emerge that after lane changing back to the automated lane downstream from the incident site, each given AC vehicle is running with a consistent speed $u_\sigma^{t_0}$ for a while; however, the disaggregated inter-vehicle spacing may be different at this moment. Such a phenomenon may exist until all the original decomposed AC vehicles have returned back to the automated lane downstream from the incident site, and then is followed by the phase of platoon reformation.

5. Platoon reforming

As seen in the title, the purpose of this phase is to reform an AC platoon while all the individual AC vehicles decomposed from a given AC platoon have returned back to the automated lane, as presented in Fig. 8, through the aforementioned incident-induced traffic control mechanisms. To accomplish this, the corresponding inter-vehicle spacing needs to be readjusted given that each presented AC vehicle has reached the preset

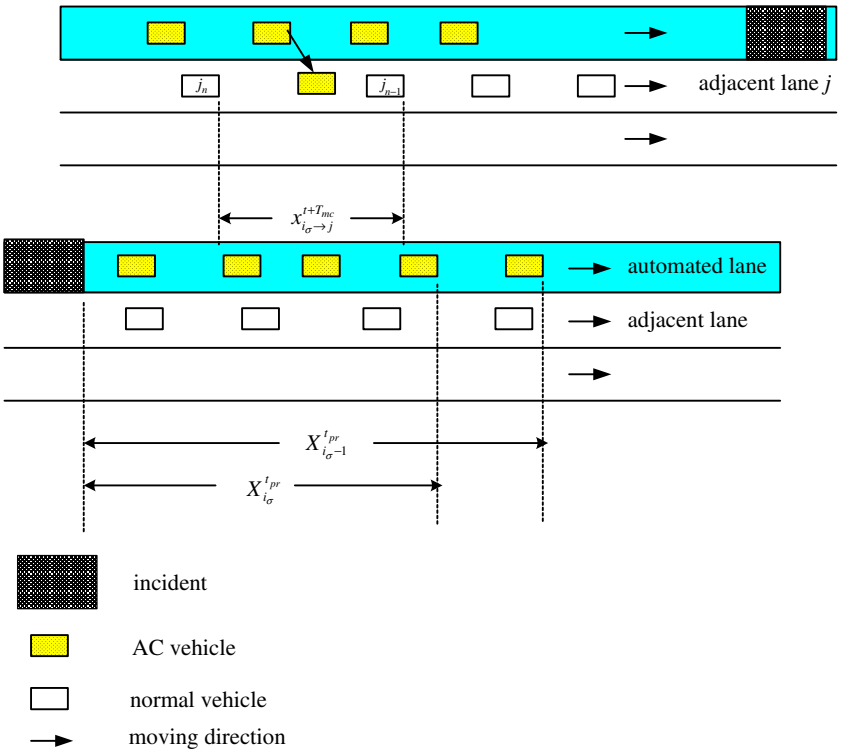

Fig. 8. Distribution of AC vehicles after completing return-lane-changing maneuvers.

platoon speed $u_{\sigma}^{t_0}$. Similarly, here we propose that the inter-vehicle spacing is adjusted in sequence, starting from the farthest upstream one, i.e., the spacing between the leading AC vehicle and the corresponding following vehicle, and the buffer time of individual spacing readjustment in the platoon reformation process (pr for short) is preset to be T_{pr}, meaning that each given spacing adjustment is completed in the interval of T_{pr}. Accordingly, the disaggregated speed adjustment rate for each given following AC vehicle to merge into the front AC platoon is derived as

$$X_{i_\sigma-1}^{t_{\mathrm{pr}}} - X_{i_\sigma}^{t_{\mathrm{pr}}} - x_\sigma^{t_0} = \frac{\alpha_{i_\sigma}^{t_{\mathrm{pr}}} \times (T_{\mathrm{pr}})^2}{2} \Rightarrow \alpha_{i_\sigma}^{t_{\mathrm{pr}}} = \frac{2(X_{i_\sigma-1}^{t_{\mathrm{pr}}} - X_{i_\sigma}^{t_{\mathrm{pr}}} - x_\sigma^{t_0})}{(T_{\mathrm{pr}})^2}, \tag{28}$$

where $\alpha_{i_\sigma}^{t_{\mathrm{pr}}}$ represents the speed adjustment rate conducted by any given AC vehicle i_σ at time t_{pr}; $X_{i_\sigma}^{t_{\mathrm{pr}}}$ and $X_{i_\sigma-1}^{t_{\mathrm{pr}}}$ refer to the instantaneous longitudinal locations of the given AC vehicle (i_σ) and the corresponding front vehicle ($i_\sigma - 1$) in the automated lane adjacent lane observed at time t_{pr}, relative downstream to the incident site; $x_\sigma^{t_0}$, as defined previously, is the preset inter-vehicle spacing of the given AC platoon (σ).

Following the aforementioned control logic, the entire platoon reformation phase is expected to be completed in the time period of $T_{\mathrm{pr}} \times (n_\sigma^{t_{\mathrm{pr}}} - 1)$.

6. Numerical results

This section summarizes the numerical results obtained from very simple simulation tests to investigate the potential performance of the proposed automated control models under various incident-induced traffic flow conditions in the single-automated-lane AHS environment. The tool utilized for preliminary tests is a specific microscopic mix-flow traffic simulation program, coded with the Turbo C language, which mimics various traffic flow conditions in the presence of automated-lane-blocking incidents in the mainline segment of a 5-km 3-lane stretch, as illustrated in Fig. 9. Herein, the proposed incident-responsive automated control

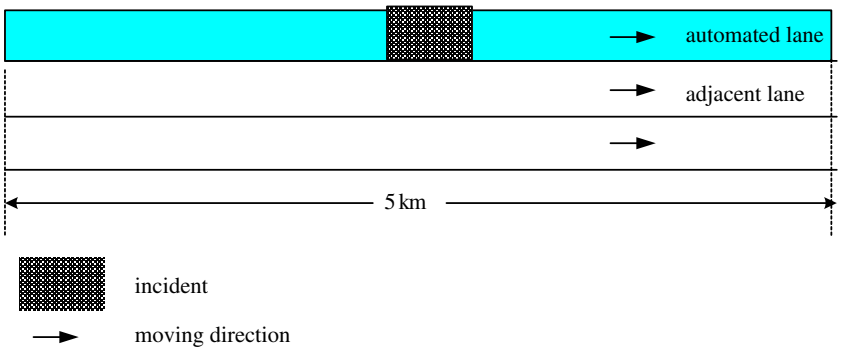

Fig. 9. Scheme of simulated study site.

models are incorporated into the developed traffic simulation program to control the movement of a given AC platoon in the process of passing by the incident site.

The primary input data and parameters preset for general traffic are summarized in Table 1. As depicted in Table 1, vehicular characteristics were predetermined, including primarily the physical size, the maximum acceleration and deceleration rates, and maximum turning angles allowed in conducting corresponding lane-changing maneuvers, e.g., mandatory lane-changing and return-lane-changing, in the presence of a given lane-blocking incident in the automated lane. Herein, all automatic vehicles are set to be private cars in the simulation. Considering the page limitation and study scope of this paper, preliminary tasks, including corresponding parameter calibration under general freeway incident conditions (i.e., human driving control conditions) using real data, are detailed elsewhere (Sheu, 2003b).

Utilizing the fundamentals and models proposed previously, a specific microscopic traffic simulation program was developed in Turbo C computer language. The framework of the proposed simulation program is shown in Fig. 10, comprising eight major subroutines which serve to deal with eight distinctive types of AC vehicular maneuvers, respectively.

The model tests aim to assess the relative performance of the proposed AC control logic and corresponding traffic behavior models under various mixed traffic flow conditions, where the initial speed and size of the approaching AC platoon, as well as diverse traffic flow conditions of the adjacent lane are considered. For comparative analyses with different combinations of parameters, we classified the test scenarios into 27 groups by the initial speed ($u_{\sigma}^{t_0}$) and size ($n_{\sigma}^{t_d}$) of the approaching AC platoon. Scenarios 1–9 are assigned to the first group where the initial AC platoon size is 2 (i.e., $n_{\sigma}^{t_d} = 2$); whereas scenarios 10–18 refer to the second group

Table 1
Summary of static characteristics of vehicles and calibrated traffic parameters

Characteristics		Length (m)	Width (m)	Top speed (km/hour)	Max. turning angle	Max. acceleration (m/second^2)	Max. deceleration (m/second^2)
Vehicle type							
Light vehicle	Car	4.0	1.6	160	45°	3.6	7.3
	Light goods vehicle (lgv.)	6.0	2.3	130	45°	2.2	7.3
Heavy vehicle	Truck	11.0	2.5	120	30°	1.4	5.6
	Bus	10.0	2.5	120	30°	1.4	5.6

Characteristics	Arrival speed (assumed to follow a normal distribution)		Expected speed (m/seconds)
	Mean value (m/seconds)	Standard deviation (m/seconds)	
Vehicle type			
Car	26.3	1.77	30.5
Lgv.	26.3	1.26	30.5
Truck	23.5	0.84	27.8
Bus	23.5	0.93	27.8

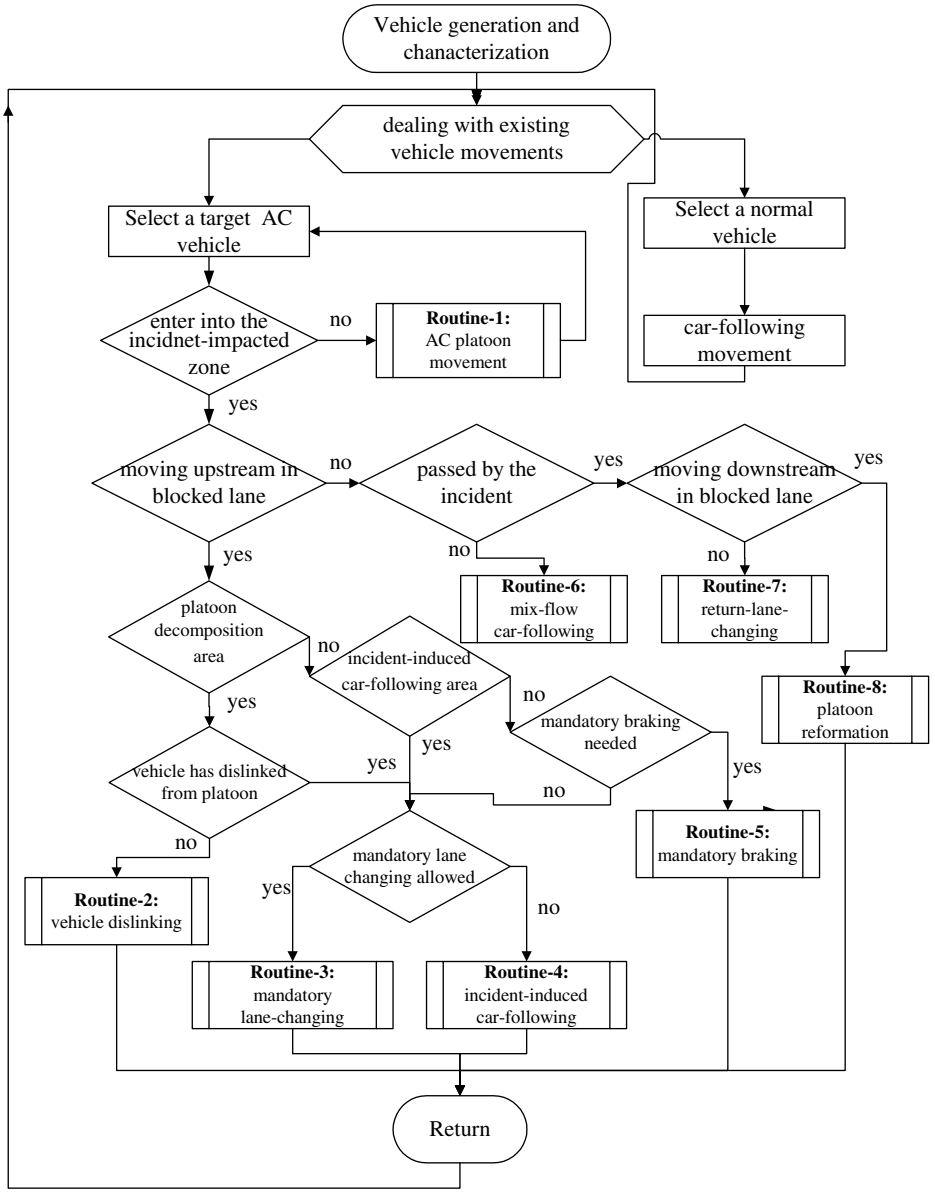

Fig. 10. Framework of the proposed microscopic traffic simulation program.

with the preset condition $n_{\sigma}^{t_d} = 5$; and scenarios 19–27 are of the third group with the preset condition $n_{\sigma}^{t_d} = 10$. In each simulation event, 10-minutes lane-blocking incidents associated with diverse traffic conditions were simulated on the middle segment of the automated lane (i.e., the inner lane). Given the aforementioned preset parameters and input data, each test scenario was simulated 10 times for aggregation of the output measures. As a consequence, there are a total of 270 simulation events involved in these tests. Table 2 presents the preset simulation characteristics.

To assess the numerical output results, four evaluation measures are utilized: (1) average AC lane travel time (AT_{AC}), (2) average AC vehicular delay (AD_{AC}), (3) average link-based travel time ($\overline{AT}$), (4) average link-based vehicular delay ($\overline{AD}$). Given the studied 5-km 3-lane mainline segment of a freeway where the inside lane is designed as a AC lane, AT_{AC} is measured by averaging the times of the simulated AC vehicles traveling in the AC lane upstream to the incident site before completing lane-changing maneuvers. Here, AT_{AC} aims to assess the performance of the proposed method in dealing with the AC vehicles queuing

Table 2
Simulation characteristics for AC platoons

Simulation characteristics	Initial AC platoon size (# of AC vehicles)	Initial approaching speed of AC platoon (kph)	Adjacent-lane traffic volume (vph)	Adjacent-lane averaged lane density (veh/km)
Scenario				
Scenario-1	2	120	500	4.9
Scenario-2	2	140	500	5.3
Scenario-3	2	160	500	5.1
Scenario-4	2	120	1000	11.7
Scenario-5	2	140	1000	12.4
Scenario-6	2	160	1000	12.7
Scenario-7	2	120	1500	20.5
Scenario-8	2	140	1500	21.4
Scenario-9	2	160	1500	22.3
Scenario-10	5	120	500	4.8
Scenario-11	5	140	500	5.2
Scenario-12	5	160	500	5.5
Scenario-13	5	120	1000	12.1
Scenario-14	5	140	1000	12.7
Scenario-15	5	160	1000	11.9
Scenario-16	5	120	1500	22.8
Scenario-17	5	140	1500	23.6
Scenario-18	5	160	1500	21.7
Scenario-19	10	120	500	4.9
Scenario-20	10	140	500	5.3
Scenario-21	10	160	500	5.6
Scenario-22	10	120	1000	12.5
Scenario-23	10	140	1000	11.8
Scenario-24	10	160	1000	12.7
Scenario-25	10	120	1500	22.1
Scenario-26	10	140	1500	21.5
Scenario-27	10	160	1500	23.2

upstream to the incident site. In the area of incident management, such an evaluation measure is critically important to assess the severity of incident-induced traffic congestion, and thus remains used in this study. The individual AC vehicular delay is defined by the difference between the time of a given AC vehicle traveling through the study site in the presence of an AC lane-blocking incident and the corresponding travel time with the initial AC platoon speed in incident-free cases. Thus, the average AC vehicular delay (AD_{AC}) can be readily estimated. In contrast, both $\overline{AT}$ and $\overline{AD}$ are two aggregate evaluation indexes aiming to evaluate the system performance of mixed traffic flows including the AC and manually-driven vehicles moving in the study site. Note that all the specified four evaluation indexes are not comparable to each other. In reality, they are respective evaluation measures specified for different assessment purposes. Using the similar measures, they can also be obtained readily from the simulation data. The numerical results of comparisons are summarized in Table 3. Several findings observed in the numerical study are provided as follows for further discussion.

Overall, the numerical results of Table 3 indicate that the proposed automatic vehicle control logic and corresponding traffic behavior models serve to respond to AC lane blockage cases. It can be found that although the AC lane traffic is affected by the lane-blocking incident, the corresponding link travel time is still lower than that of the manually-controlled traffic on the adjacent lane. Such a generalization applies to all the simulated traffic scenarios, implying that the on-site AC lane-blocking incident may not cause a significant effect on the AC vehicular throughput under the control of the proposed methodology. Furthermore, it appears that the simulated AC vehicular lane-changing and car-following maneuvers may not contribute to significant interference on the adjacent-lane traffic flow as the measured evaluation indexes do not exhibit dramatic changes given the same initial traffic flow conditions in the adjacent lane. Accordingly, it is inferred that the proposed incident-responsive automatic vehicle control methodology is promising.

Table 3
Numerical results of system performance under various traffic conditions

Evaluation criteria	AT_{AC} (seconds/AC-veh.)	AD_{AC} (seconds/AC-veh.)	$\overline{AT}$ (seconds/veh.)	$\overline{AD}$ (seconds/veh.)
Scenario				
Scenario-1	150.4	12.7	160.5	6.2
Scenario-2	138.5	16.1	160.6	6.3
Scenario-3	129.6	19.4	161.1	6.8
Scenario-4	159.1	19.1	205.4	9.0
Scenario-5	146.3	21.5	205.1	8.7
Scenario-6	137.8	25.5	206.2	9.6
Scenario-7	164.8	21.7	249.4	9.2
Scenario-8	152.8	25.6	250.3	10.1
Scenario-9	142.8	28.3	250.3	10.1
Scenario-10	159.6	20.5	168.6	9.7
Scenario-11	149.5	25.9	169.4	10.5
Scenario-12	141.7	30.4	170.3	11.4
Scenario-13	173.4	31.6	217.0	14.7
Scenario-14	163.2	37.2	217.9	15.6
Scenario-15	153.3	39.9	218.2	15.9
Scenario-16	186.3	40.5	266.0	18.8
Scenario-17	175.7	46.1	267.2	19.9
Scenario-18	164.8	48.2	267.0	19.8
Scenario-19	168.6	28.2	175.3	11.7
Scenario-20	157.5	32.7	175.9	12.4
Scenario-21	150.1	37.8	177.0	13.4
Scenario-22	182.8	39.7	225.4	17.2
Scenario-23	171.5	44.3	226.1	17.9
Scenario-24	163.6	49.1	227.6	19.4
Scenario-25	200.7	52.2	285.7	21.7
Scenario-26	190.3	58.3	287.3	23.3
Scenario-27	184.4	65.6	289.2	25.2
Average performance	161.5	34.0	217.8	13.9

In addition, there are several other noteworthy findings.

First, there seems to be a tendency that the AC lane-blockage effect on the AC traffic performance increases with either the approaching AC platoon size or time-varying adjacent-lane traffic volume. As can be seen by comparing the numerical results of scenarios 1, 10, and 19 (i.e., 12.7 seconds, 20.5 seconds and 28.3 seconds), giving the consistent AC approaching platoon speed and adjacent-lane traffic volume, the average AC link travel time appears to linearly increase with approaching AC platoon size. Such inference also applies to the other comparison cases. Accordingly, the relationships between the AC lane-blocking effects and the aforementioned two factors may warrant more investigation to improve the performance of the proposed incident-responsive automatic vehicle control system.

Second, the factor of AC approaching platoon speed seems to have a positive effect on the average AC lane travel time (i.e., AT_{AC}); however may have a negative effect on the average AC vehicular delay (AD_{AC}). According to our observations from the simulation events, higher approaching AC platoon speed may facilitate the AC vehicles moving in the AC lane, either upstream or downstream from the incident site. However, such higher AC platoon speed may impede these disaggregated AC vehicles to merge smoothly into the traffic flow in the adjacent lane, thus contributing to the increases in the corresponding travel delay. Therefore, it is also induced that the speed deviation of the approaching AC platoon relative to the aggregate traffic speed of the adjacent lane remains as a significant issue for further analyses so as to develop appropriate AC platoon speed control strategies in response to diverse lane-blocking incident cases.

Third, the adjacent-lane traffic performance seems to be affected significantly by the approaching AC platoon size relative to the factor of the approaching AC platoon speed under the condition of AC lane blockage. These are proven by comparing the corresponding numerical results of those scenarios with respect to $\overline{AT}$ and $\overline{AD}$, giving the same adjacent-lane traffic volume conditions. Such a generalization implies that the approaching AC platoon size control is vital to incident management in the AHS operational environment.

Table 4
Target parameters involved for sensitivity analyses

Target parameter	Test cases: increments of preset target parameters (%)				
	−40	−20	0	+20	+40
$A_{i_\sigma}^{mc}$ (m/seconds^2)	1.8	2.4	3.0	3.6	4.2
$D_{i_\sigma}^{mc}$ (m/seconds^2)	1.8	2.4	3.0	3.6	4.2
Θ_{mc} (deg)	27	36	45	54	63
T_{mc} (seconds)	1.8	2.4	3.0	3.6	4.2
T_d (seconds)	0.6	0.8	1.0	1.2	1.4
τ (seconds)	0.6	0.8	1.0	1.2	1.4
φ	0.06	0.08	0.1	0.12	0.14
T_{rc} (seconds)	0.6	0.8	1.0	1.2	1.4
Θ_{rc} (deg)	27	36	45	54	63
T_{pr} (seconds)	0.6	0.8	1.0	1.2	1.4

Table 5
Numerical results of sensitivity analyses

Target parameter	Test cases: increments of preset target parameters (%)				
	−40	−20	0	+20	+40
	Estimates of AT_{AC} associated with different cases (seconds/AC-veh.)				
$A_{i_\sigma}^{mc}$ (m/seconds^2)	165.9	164.4	163.2	161.8	160.3
$D_{i_\sigma}^{mc}$ (m/seconds^2)	170.6	167.5	**163.2**	161.8	158.4
Θ_{mc} (deg)	163.7	164.3	163.2	166.5	163.9
T_{mc} (seconds)	144.3	153.7	163.2	170.7	176.9
T_d (seconds)	154.6	158.5	163.2	167.9	173.3
τ (seconds)	163.4	162.9	163.2	165.8	166.4
φ	141.7	154.8	163.2	170.5	178.6
T_{rc} (seconds)	152.0	155.6	163.2	167.3	174.8
Θ_{rc} (deg)	160.3	163.9	163.2	161.5	165.2
T_{pr} (seconds)	156.7	160.4	163.2	164.8	173.4

Considering the potential effects of predetermined parameters on AC vehicular lane-changing and car-following maneuvers responding to AC lane-blocking incidents, specific sensitivity analyses were conducted. The parameters investigated in this scenario and their tentative values are summarized in Table 4. Giving the same traffic characteristics and simulation environment as that of scenario 14, these parameters were respectively tested using the measure AT_{AC}. The corresponding numerical results are summarized in Table 5.

As can be seen in Table 5, parameters, including T_{mc}, T_d, φ, T_{rc}, and T_{pr}, seem overall to have significant effects on the average AC vehicular travel time (i.e., AT_{AC}), compared to the other target parameters. Particularly, T_{mc} and T_{rc} can be regarded as two major factors influencing AC vehicular lane-changing maneuvers, where the corresponding performance in terms of AT_{AC} can be improved highly up to 18.9 seconds in the case that T_{mc} is reduced by 40%. In contrast, φ appears to be a primary factor which may reduce the corresponding performance AT_{AC} by 21.5 seconds. if the preset value of φ is reduced by 40%. This is because φ may significantly influence the dynamic safety spacing with which any given AC vehicle should remain in the process of moving in the adjacent-lane mixed traffic flow. In addition, it can also be found that the corresponding effects of all the aforementioned primary factors seem to be reversely proportional to their values. Correspondingly, giving feasible domains of parameters, the lower the corresponding values of these primary parameters are the higher the average AC travel time can be improved.

7. Concluding remarks

This paper has presented a microscopic vehicular control methodology for both automated control and investigation of potential AC vehicular maneuvers under the condition of lane-blocking incidents on the auto-

mated lane in the AHS environment. The proposed automated vehicular control logic is based on the basic safety requirements of AC vehicular movements in three corresponding sequential phases, i.e., (1) AC platoon approaching, (2) mandatory lane changing and mixed car following in the adjacent lane, and (3) AC platoon reforming downstream from the incident site in the blocked automated lane. This is followed by the development of a microscopic AC traffic simulation model which is used to simulate diverse traffic flow and control conditions for preliminary tests. aiming to investigate the relative performance of the proposed AC vehicular control models in diverse traffic flow and control conditions.

Our preliminary test results indicate that the proposed AC vehicular control logic and corresponding models are promising to deal with AC vehicles responding to diverse automated-lane blocking incident conditions with the basic safety requirements. In addition, numerical results have also implied that both the approaching AC platoon size and time-varying adjacent-lane traffic flow conditions have significant effects on the corresponding incident-responsive automated vehicle control performance, and thus warrant further investigation. Furthermore, several factors influencing AC vehicular maneuvers in terms of lane changing and car following are also noteworthy.

It is realized that automated-lane blocking incidents described in this study may not exist presently in the fully human-control traffic environments; however related issues addressed here are critical in the AHS traffic environment. Accordingly, we are presently attempting to extend the proposed methodology for both surface street incident cases and multi-automated-lane control cases. These include the uses of the proposed models in developing a network-based microscopic incident-induced traffic simulator, developing respective incident-responsive automated control logic for the multi-automated-lane AHS in response to diverse lane-blocking incident cases. Considering the robustness of the proposed control logic for more realistic scenarios (e.g., multiple AC platoons associated with different speeds, sizes, and headways, approaching to the incident site, and AC vehicles moving under the condition of non-instantaneous tracking), further effort for model extension and testing with different parameter setting scenarios is also suggested. Alternatively, the incorporation of other sophisticated methodologies such as fuzzy and stochastic modeling approaches for on-line parameter estimation is also worth considering. Furthermore, the role and corresponding effects of human factors in determining microscopic intra-lane and inter-lane AC traffic maneuvers, such as queuing and lane changing under diverse conditions of lane-blocking incidents, may also be significant issues. The possibility of other aggregate AC strategies such as platoon-based lane-changing maneuvers may also warrant more investigation as they may have certain potential advantages both in terms of time saving and the space required. Finally, research providing the link between the proposed automated incident-responsive AHS control model and AHS incident management via appropriate dispatching and transit strategies of emergency vehicles to remove incidents is greatly suggested. More importantly, it is expected that this study can stimulate more researchers' interests to depict the future of ITS in the upcoming century.

Acknowledgements

This research was supported by the grant NSC 94-2416-H-009-009 from the National Science Council of Taiwan. The author would also like to thank the referees for their constructive comments. Any errors or omissions remain the sole responsibility of the authors.

References

Broucke, M., Varaiya, 1996. A theory of traffic flow in automated highway systems. Transportation Research – Part C 4 (4), 181–210.

Chou, Y.-H., Sheu, J.-B., 1992. A simulation model of mixed traffic flow in roundabouts. Transportation Planning Journal 21 (3), 301–333.

Eskafi, F., Khorramabadi, D., Varaiya, P., 1995. An automated highway system simulator. Transportation Research – Part C 3 (1), 1–17.

Godbole, D.N., 1994. Hierarchical hybrid control of automated highway systems. Ph.D. thesis, University of California, Berkeley, USA.

Gollu, A., Varaiya, P., 1998. Smart AHS: A simulation framework for automated vehicles and highway systems. Mathematical and Computer Modeling 27 (9–11), 103–128.

Haddon, J.A., 1997. Evaluation of AHS throughput using SmartCap. In: Proceedings of the American Control Conference, Albuquerque, New Mexico, June, 1997.

Hall, R.W., Lotspeich, D., 1996. Optimized lane assignment on an automated highway. Transportation Research – Part C 4 (4), 211–229.

Hessburg, T.M., 1994. Fuzzy logic control with adaptive methods for vehicle lateral guidance. Ph.D. thesis, University of California, Berkeley, USA.

Ioannou, P., 1998. Evaluation of mixed automated/manual traffic. California PATH Research Report UCB-ITS-PRR-98-13.

Li, L., Wang, F.-Y., 2002. The automated lane-changing model of intelligent vehicle highway systems. In: Proceedings of the 5th International Conference on Intelligent Transportation Systems, September 3–6, 2002, Singapore.

Lygeros, J., Godbole, D.N., Broucke, M., 2000. A fault tolerant control architecture for automated highway systems. IEEE Transactions on Control Systems Technology 8 (2), 205–219.

Ran, B., Huang, W., Leight, S., 1996. Some solution strategies for automated highway exit bottleneck problems. Transportation Research – Part C 4 (3), 167–179.

Seto, Y., Inoue, H., 1999. Development of platoon driving in AHS. JSAE Review 20, 93–99.

Sheu, J.-B., 2002. A stochastic optimal control approach to real-time incident-responsive traffic signal control at isolated intersections. Transportation Science 36 (4), 418–434.

Sheu, J.-B., 2003a. A stochastic modeling approach to real-time prediction of queue overflows. Transportation Science 37 (1), 97–119.

Sheu, J.-B., 2003b. Simulation and real-time estimation of incident-induced traffic congestion on freeways. Project Report: NSC 91-2211-E-009-046, National Science Council, Taiwan.

Sheu, J.-B., Ritchie, S.G., 2001. Stochastic modeling and real-time prediction of vehicular lane-changing behavior. Transportation Research – Part B 35B (7), 695–716.

Sheu, J.-B., Chou, Y.-H., Shen, L.-J., 2001. A stochastic estimation approach to real-time prediction of incident effects on freeway traffic congestion. Transportation Research – Part B 35B (6), 575–592.

Toy, C., Leung, K., Alvares, L., Horowitz, R., 2002. Emergency vehicle maneuvers and control laws for automated highway systems. IEEE Transactions on Intelligent Transportation Systems 3 (2), 109–119.

Varaiya, P., 1993. Smart cars on smart roads: Problems of control. IEEE Transactions on Automatic Control 38 (2), 195–207.

Yi, J., Howell, A., Horowitz, R., Hedrick, K., Alvarez, L., 2001. Fault detection and handling for longitudinal control. California PATH Research Report UCB-ITS-PRR-2001-21.

Zhang, L., 1996. Operational models and traffic control in intelligent vehicle/highway systems. Ph.D. thesis, Princeton University, USA.